SF2A 2008
C. Charbonnel, F. Combes and R. Samadi (eds)

TURBULENT RESISTIVITY CHARACTERIZATION IN ACCRETION DISC MRI TURBULENCE.

Lesur, G.[1] and Longaretti, P-Y.[2]

Abstract. The magneto-rotational instability (MRI) is widely recognized as the most promising process to provide a turbulent transport satisfying the observational constraints. Although nearly all disk models make reference to this instability as the source of turbulence, important aspects of the MRI-driven turbulent transport properties are not well-known, in particular concerning the "resistive" transport. We have performed local simulations of the MRI to quantify this problem. We find that the resistive transport is systematically smaller than the angular momentum transport for a given configuration, and that the resistivity tensor is anisotropic.

1 Introduction

The origin of angular transport in accretion disks has always been a central problem in the disk community. The first α model (Shakura & Sunyaev 1973) already assumed a strong level of turbulence, leading to an effective viscosity orders of magnitude higher than molecular viscosity. However, the physical origin of this turbulence in disks is still largely discussed.

In a seminal paper, Balbus & Hawley (1991) have identified an MHD instability, the magnetorotational instability (MRI) that drives turbulence in the nonlinear regime. This instability has been extensively studied, mainly with local unstratified (Hawley et al. 1995) and stratified (Stone et al. 1996) 3D simulations, and global (Hawley 2000) disk simulations. These simulations have shown that MRI turbulence was an efficient way to transport angular momentum, although the role of microphysical processes was largely underestimated (Lesur & Longaretti 2007; Fromang et al. 2007).

MRI turbulence may also produce resistive transport (transport of magnetic fields) in discs. This transport is a key ingredient of accretion-ejection models (see, e.g. Ferreira 1997; Casse & Ferreira 2000 and references therein). This turbulent resistivity η_T is parameterized with the Shakura-Sunyaev ansatz as $\eta_T = \alpha_\eta v_A H$ (v_A is the Alfvén speed); stationary accretion ejection models require an anisotropy of the turbulent resistivity transport limited to a factor of order unity, and a very efficient turbulent tranport with $\alpha_\eta \lesssim 1$.

In any case, turbulent resistivity is an issue in its own right, and in this paper, we present new numerical results aimed at quantifying more precisely the resistive transport due to MRI turbulence. We first describe the physics and the numerical methods we used to study turbulence in disks. Then, we introduce the basics of the turbulent resistivity model, and we present the methodology used along with some preliminary results. Last, our findings are discussed along with some future line of work.

2 Shearing-box equations and numerical method

MRI-related turbulence has been extensively studied in the literature, and we will recall here only briefly the basic equations for the shearing-box model. The reader is referred to Hawley et al. (1995), Balbus (2003) and Regev & Umurhan (2008) for an extensive discussion of the properties and limitations of this model. Since MHD turbulence in discs is subsonic, we will work in the incompressible approximation, which allows us to eliminate

[1] Department of Applied Mathematics and Theoretical Physics, Centre for Mathematical Sciences, University of Cambridge, Wilberforce Road, Cambridge CB3 0WA, UK

[2] Laboratoire d'Astrophysique de Grenoble, UJF CNRS, BP, 53 38041 Grenoble CEDEX 9 FRANCE

sound waves and density waves. We also neglect vertical stratification, consistently with the local shearing-box model (Regev & Umurhan 2008). We include in our description a molecular viscosity and resistivity to minimize the artifacts of numerical dissipation.

The shearing-box equations are found by considering a Cartesian box centred at $r = R_0$, rotating with the disc at angular velocity $\Omega = \Omega(R_0)$ and having dimensions (L_x, L_y, L_z) with $L_i \ll R_0$. Assuming $R_0\phi \to x$ and $r - R_0 \to -y$, one eventually obtains the following set of equations for the deviations $\boldsymbol{v}$ from the local Keplerian profile:

$$\begin{aligned}
\partial_t \boldsymbol{v} + \boldsymbol{\nabla}\cdot(\boldsymbol{v}\otimes\boldsymbol{v}) &= -\boldsymbol{\nabla}\Pi + \boldsymbol{\nabla}\cdot(\boldsymbol{B}\otimes\boldsymbol{B}) - Sy\partial_x\boldsymbol{v} \\
&\quad +(2\Omega - S)v_y\boldsymbol{e_x} - 2\Omega v_x\boldsymbol{e_y} + \nu\boldsymbol{\Delta v}, \qquad (2.1)\\
\partial_t \boldsymbol{B} &= -Sy\partial_x\boldsymbol{B} + SB_y\boldsymbol{e_x} \\
&\quad +\boldsymbol{\nabla}\times(\boldsymbol{v}\times\boldsymbol{B}) + \eta\boldsymbol{\Delta B}, \qquad (2.2)\\
\boldsymbol{\nabla}\cdot\boldsymbol{v} &= 0, \qquad (2.3)\\
\boldsymbol{\nabla}\cdot\boldsymbol{B} &= 0. \qquad (2.4)
\end{aligned}$$

The boundary conditions associated with this system are periodic in the x and z direction and shearing-periodic in the y direction (Hawley et al. 1995). These equations involve the mean shear $S = -r\partial_r\Omega = (3/2)\Omega$ (a Keplerian rotation profile is assumed) . The generalized pressure term $\Pi = P/\rho_0 + \boldsymbol{B}^2/2$. Finally, the magnetic field is expressed in Alfvén-speed units, and all the velocities are given in units of SL_z. These equations are solved numerically using a Fourier Galerkin representation of (2.1)–(2.4) in a sheared frame (see Lesur & Longaretti 2005).

2.1 Turbulent resistivity definition

If MRI turbulence can be modelled as a turbulent resistivity on large scales (an assumption supported by our numerical results), one can define a large scale mean field $\bar{\boldsymbol{B}}$ and velocity $\bar{\boldsymbol{V}}$ plus fluctuating (turbulent) fields $\boldsymbol{b}$ and $\boldsymbol{v}$. We assume $\langle\boldsymbol{b}\rangle = 0$ and $\langle\boldsymbol{v}\rangle = 0$ where $\langle\rangle$ denotes an ensemble (or time, under ergodic hypothesis) average. The averaged induction equation reads:

$$\partial_t\bar{\boldsymbol{B}} = \boldsymbol{\nabla}\times(\bar{\boldsymbol{V}}\times\bar{\boldsymbol{B}}) + \nabla\times\bar{\boldsymbol{\mathcal{E}}} + \eta\Delta\bar{\boldsymbol{B}} \qquad (2.5)$$

where we have defined the mean electromotive force (EMF) $\bar{\boldsymbol{\mathcal{E}}} = \langle\boldsymbol{v}\times\boldsymbol{b}\rangle$ and we have used the definition $\langle\boldsymbol{B}\rangle \equiv \bar{\boldsymbol{B}}$ (same for $\bar{\boldsymbol{V}}$). The turbulent resistivity hypothesis assumes (in tensorial notations):

$$\bar{\mathcal{E}}_i = -\eta^T_{ik}\bar{J}_k \qquad (2.6)$$

where η^T is the (constant) turbulent resistivity tensor[1]. To confirm this model and compute turbulent resistivity coefficients, we have to find a linear correlation between the components $\bar{\mathcal{E}}_j$ and $\bar{J}_i$.

2.2 Numerical protocol

To compute the turbulent resistivity, one needs a mean current, which is not naturally present in local (shearing box) simulations. To produce this current, we have chosen to impose a large scale and *non homogeneous* field in the box. This method differs from the test field technique of Brandenburg and coworkers (see, e.g. Brandenburg et al. 2008 and references therein); the relative strengths and weaknesses of the two methods will be discussed elsewhere.

In practice, the current is produced in our Galerkin representation by forcing the largest Fourier mode in one direction to a given value B_0. To trigger the MRI, we impose a mean vertical field $B^0_z = 0.1$ for which the largest mode $k_z = 2\pi/L_z$ becomes unstable with a growth rate $\gamma \simeq S/2$. The aspect ratio is $L_x \times L_y \times L_z$=4×2×1. The factor 2 in L_y allow us to trigger more easily secondary instabilities in the strong mean vertical field cases (see Goodman & Xu 1994 and Bodo et al. 2008). The resolution used is $128\times128\times64$, similar in cell size to the one

[1] A more general relation $E_i = -\eta^T_{ijk}\partial_j B_k$ where η^T_{ijk} is an antisymmetric tensor is sometimes considered. We won't use it here for simplicity, as only one component of $\partial_j B_k$ is used at any given time.

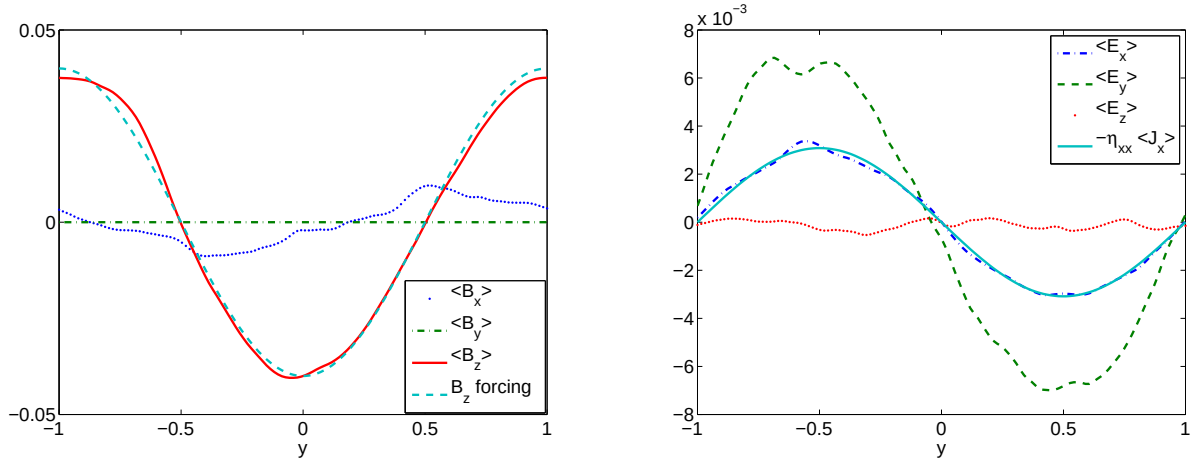

Fig. 1. Mean field (left) and emfs (right) from run ZY4 with $B_z^0 = 0.1$ and $\delta B^0 = 0.04$. We also plot the best fits corresponding to the turbulent resistivity model. We measure in this case $\eta_{xx}^T = 5.6 \times 10^{-2} SL_z^2$.

model	δB^0	$\eta_{xx}^T/(SL_z^2)$	$\eta_{yx}^T/(SL_z^2)$	$\alpha \equiv \nu^T/(SL_z^2)$
ZY1	0.01	3.6×10^{-2}	2.9×10^{-2}	1.5×10^{-1}
ZY2	0.02	3.7×10^{-2}	8.5×10^{-2}	1.5×10^{-1}
ZY3	0.03	3.6×10^{-2}	6.8×10^{-2}	1.5×10^{-1}
ZY4	0.04	2.4×10^{-2}	5.6×10^{-2}	1.3×10^{-1}
ZY5	0.08	1.1×10^{-2}	1.1×10^{-2}	7.8×10^{-2}

Table 1. Main results from the $B_z(y)$ configuration. α is the Shakura-Sunyaev like coefficient (see Lesur & Longaretti 2007 for a proper de?nition) computed from each run, and ν^T is the associated turbulent viscosity. Apart from runs ZY4 and ZY5, turbulence efficiency is constant and the turbulent Prandtl number appears to be systematically smaller than 1.

used in Lesur & Longaretti (2007). The Reynolds number is always $Re = SL_z^2/\nu = 1600$ and $Pm = \nu/\eta = 1$. Each simulation is integrated over 500 shear times, and the averages are computed from the 400 last shear times, to avoid initial conditions artefacts.

To postprocess the results, we first compute the time average $\bar{\boldsymbol{B}}$ and $\bar{\mathcal{E}}$. We then use a script which extract the mean current and compute the correlation with the emfs, giving in the end one component of the η^T tensor for one run. Note that using this procedure, we can in theory compute the resistivity associated with $B_z(y)$, $B_x(y)$ and $B_x(z)$ configurations. In this paper, we will only explore the $B_z(y)$ configuration. Similar results follow in the other configurations, and will be reported elsewhere.

3 Results

To illustrate our method we consider the following structure for the mean magnetic field (radially varying vertical field):

$$\bar{B}_z = B_z^0 + \delta B^0 \cos\left(\frac{2\pi y}{L_y}\right), \tag{3.1}$$

We show on Fig. 1 an example of a simulation result with $\delta B^0 = 0.04$. The profiles are computed from an average in time and in the (x, y) plane. From this figure, one get a classical diagonal resitivity term of $\eta_{xx}^T \sim 5.6 \times 10^{-2}$. We also find an non diagonal term $\eta_{yx}^T = 8 \times 10^{-2}$. We have repeated this kind of experience for various set of parameters, which are summarized on Tab. 1.

One may note a saturation process (models ZY4-ZY5), which may be due to the fact that increasing δB_0 to high values leads to strong modification of the background field. Since B_z^0 corresponds to the maximum of

the growth rate for the $k_z = 2\pi/L_z$ mode, this means that increasing δB^0 always weakens the instability. This explanation is confirmed by the decrease of the turbulent transport α.

According to Tab. 1, we can state that, on average

$$\eta^T_{xx} \sim 0.2\nu^T = 0.2\alpha S L_z^2. \tag{3.2}$$

In a $B_x(y)$ configuration (radially varying azimuthal field) one obtains instead $\eta^T_{zz} \sim 0.6\nu^T = 0.6\alpha S L_z^2$.

4 Conclusions

We have presented a systematic method to determine the turbulent resistivity associated with MRI turbulence in accretion discs. We have exemplified this method in the configuration of a radially varying vertical magnetic field, using nonlinear spectral simulations of turbulence. Although these results are rather preliminary, two clear trends are noticeable. First, we find that the turbulent resistivity η^T is always smaller than the turbulent viscosity ν^T. However, it is far from being negligible, and we may define a turbulent Prandtl number $Pm^T = \eta^T/\nu^T$, which is found to be of the order of 0.2—0.6. Second, we find that the turbulent resistivity is an anisotropic tensor, as expected. In particular, the toroidal field (B_x) diffuses about 3 times more rapidly than the poloidal field (B_z), in the radial direction. We also find that a non diagonal term of the turbulent resistivity tensor is non zero. As shown by Lesur & Ogilvie (2008), such terms might play an important role for disc dynamos and large scale magnetic field generation.

These results seem to suggest that the turbulent resistivity generated by the magneto-rotational instability is about and order of magnitude too weak to allow for the existence of stationary accretion-ejection structure although the anisotropy is in the right range, but further work is required to get a complete characterization of the turbulent resistivity. In particular, one needs to quantify resistivity in the presence of a vertical structure for the magnetic field. However, this configuration is not easy to compute as it excites very strong channel solutions (Goodman & Xu 1994) which leads to unphysical results. To get a more precise scaling as a function of α, one may try to vary the mean vertical field amplitude B_z^0. Although our preliminary results seem to show a good agreement with (3.2) for weaker fields, more work is required to get a complete picture. Finally, the impact of the (molecular) Prandtl number, which is known to be strong on the transport efficiency (Lesur & Longaretti 2007), is yet to be studied for the turbulent resistivity.

References

Balbus, S. A. 2003, ARA&A, 41, 555

Balbus, S. A. & Hawley, J. F. 1991, ApJ, 376, 214

Bodo, G., Mignone, A., Cattaneo, F., Rossi, P., & Ferrari, A. 2008, Accepted in A&A, 805

Brandenburg, A., Rädler, K.-H., Rheinhardt, M., & Käpylä, P. J. 2008, ApJ, 676, 740

Casse, F. & Ferreira, J. 2000, A&A, 353, 1115

Ferreira, J. 1997, A&A, 319, 340

Fromang, S., Papaloizou, J., Lesur, G., & Heinemann, T. 2007, A&A, 476, 1123

Goodman, J. & Xu, G. 1994, ApJ, 432, 213

Hawley, J. F. 2000, ApJ, 528, 462

Hawley, J. F., Gammie, C. F., & Balbus, S. A. 1995, ApJ, 440, 742

Lesur, G. & Longaretti, P-Y. 2005, A&A, 444, 25

Lesur, G. & Longaretti, P.-Y. 2007, MNRAS, 378, 1471

Lesur, G. & Ogilvie, G. I. 2008, A&A, 488, 451

Regev, O. & Umurhan, O. M. 2008, A&A, 481, 21

Shakura, N. I. & Sunyaev, R. A. 1973, A&A, 24, 337

Stone, J. M., Hawley, J. F., Gammie, C. F., & Balbus, S. A. 1996, ApJ, 463, 656